This is the accepted manuscript made available via CHORUS. The article has been published as:

Effects of stickiness on the quantum states of strongly chaotic open systems

Miguel A. Prado Reynoso, Edson M. Signor, Sandra D. Prado, and Lea F. Santos

Phys. Rev. E **110**, L062201 — Published 27 December 2024

DOI: 10.1103/PhysRevE.110.L062201

Effects of stickiness on the quantum states of strongly chaotic open systems

Miguel A. Prado Reynoso,[1] Edson M. Signor,[1] Sandra D. Prado,[2] and Lea F. Santos[1]

[1] *Department of Physics, University of Connecticut, Storrs, Connecticut 06269, USA.*
[2] *Instituto de Física, Universidade Federal do Rio Grande do Sul, Porto Alegre CP15051, Brazil.*

Focusing on the standard map of the kicked rotor, we investigate the effects of classical stickiness (orbits temporarily confined to a region of a chaotic phase space) on an open quantum system. The regions of stickiness that we identify emerge in the strongly chaotic map. By scanning the system's phase space with a leak, we show that stickiness reduces the degree of delocalization of the quantum states and the decay rate of generic initial states. We find an excellent correspondence between the classical dwell time and finite-time Lyapunov exponents with the quantum dwell time and Wehrl entropies of the quantum states. Knowledge of the structure of the classically chaotic trajectories can thus be used to determine the best placement of leaks to enhance or decrease the degree of delocalization of quantum states and to modify the quantum dynamics of open systems.

There has been increasing interest in understanding the role of chaos in open quantum systems. The analysis involves either dissipative quantum systems coupled to an environment [1–6] or the quantum counterpart of classical conservative systems, where the phase-space volume is preserved and a leak or hole is inserted [7, 8]. The dynamics of a leaky system is identical to that of the closed one until the particle escapes through the leak.

The introduction of an opening to the phase space of a chaotic classical system was first done in billiards [7]. Experimentally, there have been studies of the decay rate of ultracold atoms in optical billiards [9] and of electrons in a two-lead quantum dot [10]. Models of leaky systems have also been used in practical problems beyond billiards [11], including the loss of particles in a tokamak [12], chemical reactions [13], planetary science [14], and the morphology of the eigenstates of open quantum systems [15].

Here, we consider a leaky system and show that even in its strongly chaotic regime, it exhibits stickiness, which refers to chaotic orbits that remain in a region of the phase space for a long time before moving to large distances [16–18]. We investigate how stickiness affects the quantum states and decay rates of the quantum counterpart of the classical leaky system. The analysis focuses on the classical and quantum Chirikov standard map, that represents the discrete map of the kicked rotor [19], but the approach is general and can be applied to other strongly chaotic systems.

Stickiness was initially found around islands of stability [20], being usually associated with weakly chaotic systems, where the phase space is mixed and regions of chaotic and regular motion coexist. The applications of stickiness range from the description of anomalous diffusion [21, 22] to the arms of spiral galaxies [23]. In the case of strongly chaotic systems, phase-space inhomogeneities have been detected in leaky systems through the dependence of the escape rate on the position of the leak [24] and in closed systems via the calculation of finite-time Lyapunov exponents (FTLEs) [25], but no explicit connection was made between those inhomogeneities and stickiness.

Starting with the closed classical standard map in the strongly chaotic regime, where stability islands no longer exist, we compare the FTLEs and the recurrence times of the trajectories. We observe inhomogeneities that we associate with regions of stickiness, as suggested in [17], and explain the mechanism for this phenomenon. Specifically, the intersections of the asymptotic curves of unstable and stable manifolds can create temporary dynamical traps, that give rise to stickiness in fully chaotic systems.

Next, we introduce a leak on the phase space of the classical map and analyze how the dwell (or escape) time of the trajectories depends on the leak's position. The overall degree of chaoticity of the system increases when the leak covers regions of stickiness.

To explore how the position of the leak affects the properties of the quantum system, we analyze the decay rate of the norm of generic initial states, the lifetime of the eigenstates of the propagator, the Husimi functions of the Schur states (orthonormalized eigenstates), and their phase-space (Wehrl) entropy. We find excellent correspondence between the phase-space distribution of the classical trajectories and the Husimi functions of the Schur states. There is also agreement on the dependence of the quantum and classical quantities on the leak's position. When the leak covers regions of stickiness, increasing the FTLEs, the Wehrl entropy grows, indicating that the quantum states become more delocalized. Simultaneously, the classical and quantum dwell times decrease and the classical (quantum) decay rate of the survival probability of the trajectories (of the norm of generic quantum states) increases.

Quantum scars [26, 27], supersharp resonances [28, 29], and the fractal Weyl law [30] have been extensively investigated. Scars, in particular, have received increasing attention in the context of many-body quantum systems [31]. In contrast, the effects that stickiness from fully chaotic classical systems can have on the localization and dynamics of quantum systems have hardly been explored. Our work closes this gap and stimulates further analyses of how phase-space structures can impact

both closed and open quantum systems.

Closed classical and quantum models.– We consider the paradigmatic standard map for which the classical dynamics and the quantization via Floquet theory are well established. This stroboscopic map describes the Poincaré section of a rotor that is periodically kicked and moves freely between kicks. It is given by $q_{n+1} = q_n + p_n$, $p_{n+1} = p_n - \frac{K}{2\pi}\sin(2\pi q_{n+1})$, where the canonical conjugated coordinates q_n and p_n are taken mod 1. Time is then counted in terms of the number of iterations of the map. The stochastic parameter K in the equation above is chosen as $K = 10$ to ensure strong chaos. At this value of K, there are no visible islands of regularity.

Due to the toroidal phase space $\mathbb{T}^2$, the quantization of the standard map leads to a finite Hilbert space of dimension $N = 2\pi/\hbar$ with a discretized position basis $q = k/N$ and $k = 1, \ldots, N$. In this basis, the time-evolution operator after one iteration is

$$U_{k,k'} = \frac{1}{\sqrt{N}} \exp\left\{\frac{i\pi}{N}(k-k')^2 + \frac{iNK}{2\pi}\cos\left(\frac{2\pi}{N}k\right)\right\}. \quad (1)$$

Stickiness in the closed chaotic classical system.– In Fig. 1(a), we present a density plot of the FTLEs computed after $n = 10$ iterations of the closed classical map. FTLEs provide a local measure of the exponential divergence of phase-space trajectories over a finite time interval [32–39] and allow for the detection of phase-space structures [40–43]. Despite the strongly chaotic regime ($K = 10$), the phase space of the map reveals regions with notably lower FTLEs (dark blue) than the surrounding areas (ranging from green to yellow).

Chaos emerges near unstable periodic orbits, driven by the intersections of asymptotic curves. The regions of lower FTLE values identified in Fig. 1(a) offer insights into the geometry of these asymptotic curves. The two shaded rectangular strips, centered at $\overline{q}_L = 0.2$ and at $\overline{q}_L = 0.5$, highlight distinct structures of the phase space. The strip at $\overline{q}_L = 0.2$ shows intricate regions of folded curves, while the strip at $\overline{q}_L = 0.5$ displays more uniform regions dominated by straighter lines. Complementing this analysis, we plot in Fig. 1(b) the average local angle between the asymptotic curves of unstable and stable manifolds over $n = 10$ iterations using the same initial conditions as in Fig. 1(a) [44]. We see that the regions of low FTLEs correspond to small angles. Therefore, the origin of these regions lies in the decreased degree of hyperbolicity associated with asymptotic curves that are quasi-tangential [Fig. 1(b)] and in the high density of folds, as in the strip at $\overline{q}_L = 0.2$ in Fig. 1(a). This complex geometry traps the chaotic orbits and justifies the term "stickiness".

To quantify the effect of stickiness, we compute the statistics of the number of times a trajectory returns to the area of its initial condition centered at a tiny radius $r = 10^{-3}$. Each initial condition, over a sample of 10^8 random choices in a strip of length 0.2, is evolved for $n = 10$ iterations. In Fig. 1(c), we show the total number of recurrences, denoted by T_r, as a function of the strip's position $\overline{q}_L$. The largest values of T_r correlate with the small FTLEs in Fig. 1(a) and the small angles in Fig. 1(b).

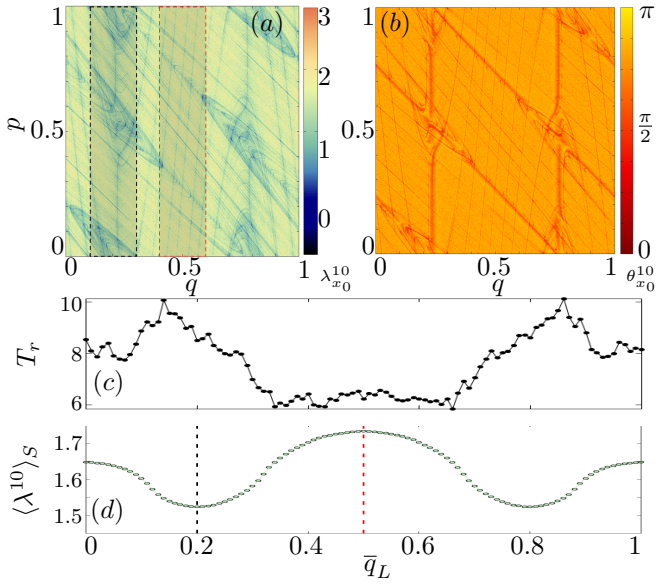


FIG. 1. Density plot of (a) the finite-time Lyapunov exponents (FTLEs) and -(b) the average local angle between unstable and stable manifolds for different initial conditions of the closed classical standard map after $n = 10$ iterations. (c) Number of recurrences over 10^8 random initial conditions within a strip of length $\Delta q = 0.2$ centered at $\overline{q}_L$. Each initial condition is evolved for $n = 10$ iterations and we count the number of times a trajectory returns to a distance less than $r = 10^{-3}$ from its initial condition. (d) Mean value of the FTLEs for initial conditions in a strip of width $\Delta q = 0.2$ centered at $\overline{q}_L$. In (a): Two strips are illustrated with shaded areas, one centered at $\overline{q}_L = 0.2$ and the other at $\overline{q}_L = 0.5$.

The number of recurrences in Fig. 1(c) is also closely related with the average values of the FTLEs shown in Fig. 1(d), which are computed within a strip of length $\Delta q = 0.2$ centered at position x_q,

$$\langle\lambda^{10}\rangle_S = \frac{1}{\mu_S}\int_S d\mu\ \lambda^{10}_{\boldsymbol{x}_0}, \quad (2)$$

where $\boldsymbol{x}_0 = (q_0, p_0)$ denotes the initial condition and μ_S represents the measure on the region S of the strip. We mark with vertical dashed lines the two regions that we select for further analysis: $\overline{q}_L = 0.2$, where $\langle\lambda^{10}\rangle_S$ is small, and $\overline{q}_L = 0.5$, where $\langle\lambda^{10}\rangle_S$ is large.

Leaking classical system.– The strips illustrated in Fig. 1(a) become now leaks. The map recursion remains the same as in the closed system until (q_n, p_n) falls into the leak and the trajectory is halted. The time that the trajectory for a given initial condition remains in the phase space is the classical dwell time, τ. The FTLE

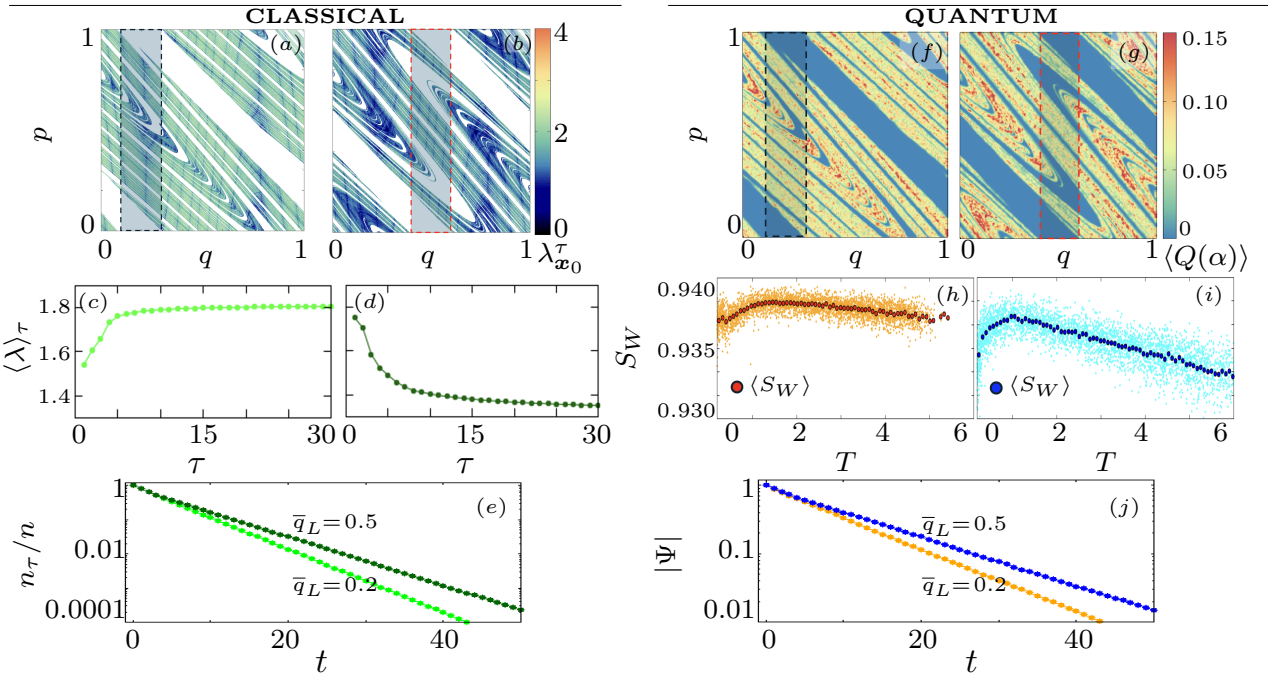


FIG. 2. Leaking (a)-(e) classical and (f)-(j) quantum system with a leak at (a,c,f,h) $\overline{q}_L = 0.2$ and (b,d,g,i) $\overline{q}_L = 0.5$. (a)-(b) FTLEs, $\lambda^{\tau}_{\boldsymbol{x}_0}$, for various initial conditions $\boldsymbol{x}_0$. Regions in white correspond to trajectories discarded due to their small dwell times. (c)-(d) Average FTLE as a function of the classical dwell time. (e) Survival probability of trajectories for 10^8 uniformly distributed initial conditions. (f)-(g) Husimi functions averaged over 20 Schur states with the largest dwell times to avoid leak-correlated states with fluctuating values of S_W. (h)-(i) Wehrl entropies of the Schur vectors as a function of the quantum dwell times. Light circles indicate S_W and dark circles indicate the average, $\langle S_W\rangle$, over intervals of $\Delta T = 0.08$; $N = 10^4$ and Husimi's resolution of 10^6. (j) Decay of the norm of an initial state constructed from a random superposition of the eigenstates of a random unitary matrix of the circular unitary ensemble.

associated with that initial condition is determined up to τ and is denoted by $\lambda^{\tau}_{\boldsymbol{x}_0}$.

In Figs. 2(a)-(b), we show the density plots for the FTLEs of the open classical map, $\lambda^{\tau}_{\boldsymbol{x}_0}$, obtained for various different initial conditions. White regions correspond to trajectories with small dwell time, which are discarded, because they do not follow the universal exponential decay of the survival probability, that is, for such short times, the ratio between the number of trajectories that remain in the phase space and the total number of initial conditions does not decay exponentially in time [8].

Motivated by the results in Fig. 1, the leak in Fig. 2(a) is centered at $\overline{q}_L = 0.2$ to eliminate a region of the phase-space with predominance of stickiness, while the leak at $\overline{q}_L = 0.5$ in Fig. 2(b) covers a region with almost no sign of stickiness. As a consequence, the values of the FTLEs in Fig. 2(a) are larger (green to yellow) than the FTLEs (dark blue) in Fig. 2(b).

To provide more detail on how the degree of chaos depends on the position of the leak, we compute the average FTLE, $\langle\lambda\rangle_\tau$, for trajectories with dwell time τ. In Fig. 2(c) [Fig. 2(d)], we show the average FTLE as a function of τ for the leak at $\overline{q}_L = 0.2$ [$\overline{q}_L = 0.5$]. The first trajectories to escape are those close to the leak. When the leak is [not] on the region of stickness, as in Fig. 2(c) [Fig. 2(d)], those trajectories have low [high] FTLE, so $\langle\lambda\rangle_\tau$ is small [large] for small τ. The opposite happens for long dwell times, where the surviving trajectories in Fig. 2(c) are more chaotic leading to larger average FTLE than in Fig. 2(d).

Leaking quantum system.– The propagator $\tilde{U}$ of the open quantum map is nonunitary. It is obtained by projecting the unitary propagator U of the closed system in Eq. (1) on the complement of the leak, $\tilde{U} = \Pi U$. Since the leak is a strip parallel to the p axis, the projector Π is diagonal in the position representation. The eigenvalues of $\tilde{U}$ are $z_k = \exp\{i\theta_k - \Gamma_k/2\}$, where θ_k is the quasiangle and Γ_k is the uniform decay rates of each quantum state, with $T_k = 1/\Gamma_k$ denoting their dwell time.

The eigenstates of $\tilde{U}$, known as resonances, form a nonorthogonal set in which left and right eigenvectors are different, the former being linked to the backward propagation and the latter to the forward propagation of the system. Since these states are not orthonormal, they can overlap, which prevents resolution of the classical trajectories. We use the Schur decomposition [45, 46] to obtain an orthonormal set. The Schur vectors properly discriminate the regions of the phase space corresponding to the dwell times of the resonances [46, 47], thus ensuring a proper semiclassical analyses.

In Figs. 2(f)-(g), we show density plots of the Husimi functions, $Q_k(\alpha) = \exp\{-2\pi N|\alpha|^2\}|\langle\alpha|v_k\rangle|^2$, which give the distribution of a Schur state $|v_k\rangle$ in the phase space, with $|\alpha\rangle$ being a coherent state centered at $(q,p) \in \mathbb{T}^2$. As in Fig. 2(a) [Fig. 2(b)], the leak in Fig. 2(f) [Fig. 2(g)] is at position $\overline{q}_L = 0.2$ [$\overline{q}_L = 0.5$]. There is a clear parallel between the classical and quantum results, with regions of low hyperbolicity (dark blue) in Figs. 2(a)-(b) being mirrored by regions of increased localization (red) of the quantum system in Figs. 2(f)-(g).

To measure the degree of delocalization of the Schur states in phase space, we compute the Wehrl entropy [48],

$$S_W^{(k)} = -\frac{1}{\mathcal{N}} \int d\alpha \, Q_k(\alpha) \ln Q_k(\alpha), \tag{3}$$

where $\mathcal{N}$ is a normalization constant and $0 \leq S_W \leq 1$. A fully delocalized state has $S_W = 1$, and the uttermost localized state has $S_W = 0$. Analogously to the classical Figs. 2(c)-(d), the quantum Figs. 2(h)-(i) display the Wehrl entropies of the Schur states with respect to the dwell times T. Light circles correspond to the entropy for a single state, S_W, and dark circles give the average, $\langle S_W\rangle$, over states in an interval $\Delta T = 0.08$. Comparable to the classical results in Figs. 2(c)-(d), when we get rid of stickiness by placing the leak at $\overline{q}_L = 0.2$ in Fig. 2(h), both S_W and $\langle S_W\rangle$ reach larger values, indicating a greater degree of delocalization, than in Fig. 2(i), where $\overline{q}_L = 0.5$.

Classical and quantum dynamics.– To investigate the effect of stickiness on phase space dynamics, we evolve the trajectories for a uniform density of $n = 10^8$ randomly chosen initial conditions covering the entire phase space. At each iteration, we calculate the number of initial conditions that remain in the phase space, n_τ. In Fig. 2(e), we show the ratio n_τ/n as a function of τ for $\overline{q}_L = 0.2$ (light green) and $\overline{q}_L = 0.5$ (dark green). When the stickiness region is removed with $\overline{q}_L = 0.2$, the escape rate of the trajectories increases significantly.

Interestingly, we verify in Fig. 2(j) that stickiness associated with the structures of classical manifolds also influences quantum dynamics. We evolve an initial state, Ψ_0, that randomly covers the entire phase space and calculate its norm $|\Psi_0|$. The decay rate of the norm is smaller in the presence of stickiness [$\overline{q}_L = 0.5$ (blue)] than in its absence [$\overline{q}_L = 0.2$ (orange)].

Classical-quantum correspondence.– Figure 3 provides a general picture of the correlation between stickiness and the properties of leaking systems. Exhibiting excellent classical-quantum correspondence, the average classical dwell time in Fig. 3(a) and the average quantum dwell time in Fig. 3(b) decrease when the leak removes a region of stickiness, that is, $\langle\tau\rangle$ and $\langle T\rangle$ reach their smallest values for leaks placed in the vicinity of $\overline{q}_L = 0.2$ and $\overline{q}_L = 0.8$ (cf. Fig. 1). Likewise, the average FTLE in Fig. 3(c) and the average Wehrl entropy in Fig. 3(d) increase when stickiness is eliminated. In Fig. 3(b), we

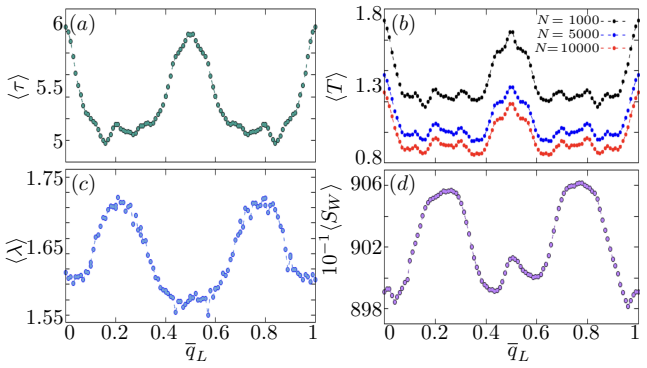


FIG. 3. Classical-quantum correspondence and dependence on the position $\overline{q}_L$ of the leak. (a) Classical dwell time and (c) FTLE, both averaged over all points of the phase space, as a function of $\overline{q}_L$. (b) Quantum dwell time and (d) Wehrl entropy, both averaged over all N Husimi-Schur vectors, as a function of $\overline{q}_L$. In (b): Three different Hilbert space sizes are considered. In (d): $N = 5000$ and Husimi's resolution of 10^6.

display results for different Hilbert space sizes, N. The dependence on the position of the leak remains the same, and the values of $\langle T\rangle$ converge as N increases.

Conclusions.– Typically, the phase space of hard-chaotic systems does not present structures. Yet, our analysis of the strongly chaotic classical standard map revealed the presence of stickiness. We verified that the mechanism for this new type of stickiness affects not only the properties of the classical system, but also the dynamics of its quantum counterpart. Similarly to the notion of unstable periodic orbits getting imprinted in the quantum states in the form of quantum scars, the structure of the manifolds can leave its mark on the quantum system. But contrary to quantum scars, whose effects are restricted, since they have measure zero, stickiness exists in finite regions of the phase space.

When the leak is placed on a region of stickiness, removing its influence, the overall degree of chaoticity of the classical system increases. In this case, the average finite-time Lyapunov exponents (classical dwell times) increase (decrease) and the trajectories escape faster. These changes are directly manifested in the quantum system, where the degree of delocalization (quantum dwell times) of the quantum states also increase (decrease) and the decay rate of initial states grows. These results imply that by properly choosing where to place a leak in the classical phase space, one can control the level of delocalization and dynamics of a quantum system.

Our method for detecting and analyzing the effects of stickiness can be extended to other leaky or dissipative systems in the strongly chaotic regime. Stickiness is one more element worth attention in current studies of chaos, localization, and dynamics in open quantum systems.

Acknowledgments.– This research was supported by the NSF CCI grant (Award Number 2124511).

[1] I. Rotter, A non-Hermitian Hamilton operator and the physics of open quantum systems, J. Phys. A **42**, 153001 (2009).

[2] G. Akemann, M. Kieburg, A. Mielke, and T. Prosen, Universal signature from integrability to chaos in dissipative open quantum systems, Phys. Rev. Lett. **123**, 254101 (2019).

[3] R. Hamazaki, K. Kawabata, and M. Ueda, Non-Hermitian many-body localization, Phys. Rev. Lett. **123**, 090603 (2019).

[4] D. Villaseñor, L. F. Santos, and P. Barberis-Blostein, Breakdown of the quantum distinction of regular and chaotic classical dynamics in dissipative systems (2024), arXiv:2406.07616 [quant-ph].

[5] A. M. García-García, J. J. M. Verbaarschot, and J. ping Zheng, The Lyapunov exponent as a signature of dissipative many-body quantum chaos (2024), arXiv:2403.12359 [hep-th].

[6] L. Sá, Signatures of dissipative quantum chaos (2023), arXiv:2311.01518 [cond-mat.stat-mech].

[7] G. Pianigiani and J. A. Yorke, Expanding Maps on Sets Which are Almost Invariant: Decay and Chaos, Trans. Am. Math. Soc. **252**, 351 (1979).

[8] E. G. Altmann, J. S. E. Portela, and T. Tél, Leaking chaotic systems, Rev. Mod. Phys. **85**, 869 (2013).

[9] N. Friedman, A. Kaplan, D. Carasso, and N. Davidson, Observation of Chaotic and Regular Dynamics in Atom-Optics Billiards, Phys. Rev. Lett. **86**, 1518 (2001).

[10] C. M. Marcus, R. M. Westervelt, P. F. Hopkins, and A. C. Gossard, Phase breaking in ballistic quantum dots: Experiment and analysis based on chaotic scattering, Phys. Rev. B **48**, 2460 (1993).

[11] J. Nagler, M. Krieger, M. Linke, J. Schönke, and J. Wiersig, Leaking billiards, Phys. Rev. E **75**, 046204 (2007).

[12] J. S. Portela, I. L. Caldas, and R. L. Viana, Tokamak magnetic field lines described by simple maps, EPJ ST **165**, 195 (2008).

[13] R. S. Dumont and P. Brumer, Decay of a chaotic dynamical system, Chem. Phys. Lett. **188**, 565 (1992).

[14] J. Nagler, Crash test for the Copenhagen problem, Phys. Rev. E **69**, 066218 (2004).

[15] L. Ermann, G. G. Carlo, and M. Saraceno, Localization of Resonance Eigenfunctions on Quantum Repellers, Phys. Rev. Lett. **103**, 054102 (2009).

[16] G. Contopoulos and M. Harsoula, Stickiness in Chaos, Int. J. Bifurc. Chaos **18**, 2929 (2008).

[17] G. Contopoulos and M. Harsoula, Stickiness Effects in Conservative Systems, Int. J. Bifurc. Chaos **20**, 2005 (2010).

[18] R. Dvorak, "Stickiness" in Dynamical Systems, in *The Dynamics of Small Bodies in the Solar System: A Major Key to Solar Systems Studies*, edited by B. A. Steves and A. E. Roy (Springer Netherlands, Dordrecht, 1999) pp. 509–534.

[19] B. V. Chirikov, A universal instability of many-dimensional oscillator systems, Phys. Rep **52**, 263 (1979).

[20] G. Contopoulos, Orbits in Highly Perturbed Dynamical Systems. 111. Nonperiodic Orbits, Astron. J. **76**, 147 (1971).

[21] A. L. Livorati, M. S. Palmero, G. Díaz-I, C. P. Dettmann, I. L. Caldas, and E. D. Leonel, Investigation of stickiness influence in the anomalous transport and diffusion for a non-dissipative Fermi-Ulam model, Commun. Nonlinear Sci. Numer. Simul. **55**, 225 (2018).

[22] D. Borin, A. L. P. Livorati, and E. D. Leonel, An investigation of the survival probability for chaotic diffusion in a family of discrete Hamiltonian mappings, Chaos, Solitons & Fractals **175**, 113965 (2023).

[23] N. Voglis, P. Tsoutsis, and C. Efthymiopoulos, Invariant manifolds, phase correlations of chaotic orbits and the spiral structure of galaxies, Mon. Not. R. Astron. Soc **373**, 280 (2006).

[24] L. A. Bunimovich and A. Yurchenko, Where to place a hole to achieve a maximal escape rate, Isr. J. Math. **182**, 229–252 (2011).

[25] K. Yoshida, H. Yoshino, A. Shudo, and D. Lippolis, Eigenfunctions of the Perron–Frobenius operator and the finite-time Lyapunov exponents in uniformly hyperbolic area-preserving maps, J. Phys. A **54**, 285701 (2021).

[26] E. J. Heller, Bound-state eigenfunctions of classically chaotic Hamiltonian systems: Scars of periodic orbits, Phys. Rev. Lett. **53**, 1515 (1984).

[27] S. Pilatowsky-Cameo, D. Villaseñor, M. A. Bastarrachea-Magnani, S. Lerma-Hernández, L. F. Santos, and J. G. Hirsch, Ubiquitous quantum scarring does not prevent ergodicity, Nat. Comm. **12**, 852 (2021).

[28] M. Novaes, Supersharp resonances in chaotic wave scattering, Phys. Rev. E **85**, 036202 (2012).

[29] M. Novaes, Resonances in open quantum maps, J. Phys. A **46**, 143001 (2013).

[30] D. L. Shepelyansky, Fractal Weyl law for quantum fractal eigenstates, Phys. Rev. E **77**, 015202 (2008).

[31] C. J. Turner, A. A. Michailidis, D. A. Abanin, M. Serbyn, and Z. Papić, Weak ergodicity breaking from quantum many-body scars, Nat. Phys. **14**, 745 (2018).

[32] G. You and S. Leung, Computing the finite time Lyapunov exponent for flows with uncertainties, J. of Comp. Phys. **425**, 109905 (2021).

[33] K. P. K Stefański, K. Buszko, Transient chaos measurements using finite-time Lyapunov exponents, Chaos **20**, 033117 (2010).

[34] E. H.-G. G. Drótos and C. López, Local characterization of transient chaos on finite times in open systems, J. Phys. Complex **2**, 025014 (2021).

[35] A. Prasad and R. Ramaswamy, Characteristic distributions of finite-time Lyapunov exponents, Phys. Rev. E **60**, 2761 (1999).

[36] T. Manos and M. Robnik, Statistical properties of the localization measure in a finite-dimensional model of the quantum kicked rotator, Phys. Rev. E **91**, 042904 (2015).

[37] M. A. Prado Reynoso, G. J. Delben, M. Schlesinger, and M. W. Beims, Finite-time Lyapunov fluctuations and the upper bound of classical and quantum out-of-time-ordered expansion rate exponents, Phys. Rev. E **106**, L062201 (2022).

[38] L. Storm, H. Linander, J. Bec, K. Gustavsson, and B. Mehlig, Finite-time Lyapunov exponents of deep neural networks, Phys. Rev. Lett. **132**, 057301 (2024).

[39] E. Ott, *Chaos in Dynamical Systems* (Cambridge University Press, Cambridge, UK, 2002).

[40] G. Lapeyre, Characterization of finite-time Lyapunov exponents and vectors in two-dimensional turbulence, Chaos **12**, 688 (2002).

[41] M. R. Sales, M. Mugnaine, J. Szezech, R. L. Viana, N. M. Ibere Caldas, and J. Kurths, Stickiness and recurrence

plots: An entropy-based approach, Chaos **33**, 033140 (2023).
[42] M. A. Prado Reynoso and M. W. Beims, Studying finite-time (non)-domination in dynamical systems using Oseledec's splitting. application to the standard map, Commun. Nonlinear Sci. Numer. Simul. **110**, 106358 (2022).
[43] S. C. Shadden, F. Lekien, and J. E. Marsden, Definition and properties of lagrangian coherent structures from finite-time Lyapunov exponents in two-dimensional aperiodic flows, Physica D **212**, 271 (2005).
[44] These angles are derived using the covariant Lyapunov vectors [42, 49, 50].
[45] H. Schomerus and J. Tworzydło, Quantum-to-Classical Crossover of Quasibound States in Open Quantum Systems, Phys. Rev. Lett. **93**, 154102 (2004).
[46] J. Hall, S. Malzard, and E.-M. Graefe, Semiclassical Husimi Distributions of Schur Vectors in Non-Hermitian Quantum Systems, Phys. Rev. Lett. **131**, 040402 (2023).
[47] M. Kopp and H. Schomerus, Fractal Weyl laws for quantum decay in dynamical systems with a mixed phase space, Phys. Rev. E **81**, 026208 (2010).
[48] A. Wehrl, General properties of entropy, Rev. Mod. Phys. **50**, 221 (1978).
[49] F. Ginelli, P. Poggi, A. Turchi, H. Chaté, R. Livi, and A. Politi, Characterizing dynamics with covariant lyapunov vectors, Phys. Rev. Lett. **99**, 130601 (2007).
[50] M. A. P. Reynoso, R. M. da Silva, and M. W. Beims, Studying partial hyperbolicity inside regimes of motion in hamiltonian systems, Chaos, Solitons & Fractals **144**, 110640 (2021).